HHS Public Access

Author manuscript

Brain Stimul. Author manuscript; available in PMC 2019 July 01.

Published in final edited form as:

Brain Stimul. 2018 ; 11(4): 689–698. doi:10.1016/j.brs.2018.01.034.

Non-invasive vagus nerve stimulation reduces blood-brain barrier disruption in a rat model of ischemic stroke

Yirong Yang[b], **Lisa Y. Yang**[a], **Lilla Orban**[a], **Darnell Cuylear**[a], **Jeffrey Thompson**[a], **Bruce Simon**[c], and **Yi Yang**[a,*]

[a]Department of Neurology, University of New Mexico Health Sciences Center, Albuquerque, NM 87131, USA

[b]College of Pharmacy, University of New Mexico Health Sciences Center, Albuquerque, NM 87131, USA

[c]ElectroCore LLC, Basking Ridge, NJ 07920, USA

Abstract

Background—Vagus nerve stimulation (VNS) significantly reduces infarct volume in rat models of cerebral ischemia, but the mechanism of this protective effect remains open.

Hypothesis—This study tested the hypothesis that non-invasive VNS (nVNS), during transient middle cerebral artery occlusion (MCAO), protects the blood-brain barrier (BBB), leading to reduced infarct size in ischemic brain.

Methods—Spontaneous hypertensive rats (SHRs) were subjected to a 90 min MCAO. nVNS treated rats received 5 stimulations (duration: 2min; every 10 min) on the skin overlying the cervical vagus nerve in the neck beginning 30 min after MCAO onset. Control rats received the same stimulations on the quadriceps femoris muscle. Twenty-four hours after MCAO onset, MRI and immunohistochemistry (IHC) were performed for analyses of infarct size and BBB leakage.

Results—Compared with the control group, anatomic MRI T2-weighted images showed significantly smaller infarct sizes in the nVNS group. Dynamic contrast-enhanced (DCE)-MRI showed a significantly decreased BBB transfer rate (Ki map) in the lesion area in the nVNS group, which was spatially correlated with the attenuation of the infarct size. Furthermore, significantly lower serum IgG leakage, visualized by IHC, was seen in the ischemic hemisphere in nVNS treated rats. nVNS also protected vascular tight junction proteins from disruption in microvessels,

*Corresponding author. Department of Neurology, MSC11 6035, 1 University of New Mexico, Albuquerque, NM 87131-0001, USA. yyang@salud.unm.edu (Y. Yang).

Disclosures

Dr. Bruce Simon is an employee with electroCore LLC.

Conflicts of interest

All authors declare no conflict of interest.

Ethical approval

All applicable national and institutional guidelines for the care and use of animals were followed. This article does not contain any studies with human participants performed by any of the authors.

and reduced expression of matrix metalloproteinases-2/9 in reactive astrocytes surrounding the compromised vessels in the ischemic hemispheres.

Conclusion—Our data suggest that the neuroprotective role of a series of nVNS administrations during MCA occlusion, spatially correlates with protection of BBB integrity from damage and reduction of infarct extent induced by ischemic stroke.

Keywords

MCAO; Vagus nerve stimulation; BBB permeability; MRI; MMPs; Tight junction proteins

Introduction

Treatment options for cerebral ischemic stroke are limited, since ischemia-induced brain injury is a complex and multiple stage process. During the early stages of occlusion and reperfusion, providing interventions to protect brain from injury could significantly improve neurological outcome [1,2]. However, thrombolysis with recombinant tissue plasminogen activator (t-PA), the only currently approved acute treatment for ischemic stroke, is limited by a short treatment time window, low rates of reperfusion, the potential for hemorrhagic transformation, and neurotoxicity. There is an urgent need for new acute stroke therapies.

Electrical stimulation of the left cervical vagus nerve is an FDA-approved adjunctive therapy for partial epilepsy and drug-resistant depression and has been used clinically since 1997 [3]. Vagus nerve stimulation (VNS) is also a potential therapy for migraine, Alzheimer's disease, and traumatic brain injury [4–7] and has been suggested to provide protection against ischemic brain injury [5,8]. Recently, a non-invasive VNS (nVNS) device was FDA approved for the acute treatment of cluster headache in episodic patients [9]. Ay et al. have shown that a nVNS approach, initiated 30 min after a transient middle cerebral artery occlusion (MCAO), reduces infarct volume by approximately 33% in a rat model on day 7 after reperfusion [10]. In addition, nVNS inhibits ischemia-induced immune activation and reduces functional deficit in rats without causing cardiac or hemodynamic adverse effects when initiated up to 4 h after MCAO. These observations suggest that nVNS may provide a novel, non-pharmacologic, neuroprotective treatment for acute ischemic brain injury.

The anti-inflammatory properties of the vagus nerve may suggest an important mechanism underling the neuroprotective role of VNS via activation of the splenically-mediated sympathetic anti-inflammatory pathway involving acetylcholine (ACh) and α-7-nicotinic ACh receptors [4,11,12]. MCAO-induced spleen size reduction has been correlated with ischemic volume and with changes in serum pro-inflammatory cytokine levels [13]. However, the ischemic stroke induced increase of pro-inflammatory cytokines in serum was only seen after 6 h of MCAO onset, while the neuroprotective time window of nVNS was only up to 4 h after the induction of ischemia [10], suggesting other mechanisms. During cerebral ischemia, blood-brain barrier (BBB) disruption is a critical event leading to vasogenic edema, neuroinflammation, and secondary brain injury [1,14]. We previously demonstrated that BBB disruption occurs early enough to be within the thrombolytic time window in a MCAO model in rat [15]. We have also shown that matrix metalloproteinases (MMP)-2 and –9 contribute to early ischemic BBB damage by triggering tight junction

proteins (TJP) disruption [15,16]. In this study, we tested the hypothesis that performing nVNS at an early stage of occlusion of MCA protects the BBB, resulting in reduced infarct size in the ischemic brain. To be clinically relevant, a non-invasive VNS approach was applied to rats subjected to a transient MCAO [10,17–19] due to the impracticality of implanting a vagus nerve stimulator in an acute stroke patient. It is the hope that the nature of the non-invasive, transcutaneous VNS could provide the potential for easier clinical translation [20]. We investigated the spatiotemporal correlation of protection of BBB from damage by nVNS with reduction of ischemic infarct size by using MRI approaches, as well as with the expression of TJPs and MMP-2/9 in vascular endothelial cells (EC) and astrocytes (AC) with immunohistochemistry.

Methods

Middle cerebral artery occlusion (MCAO) and vagal nerve stimulation

The study (including animal use, magnetic resonance imaging (MRI) procedures, and nVNS treatment) was approved by the University of New Mexico Animal Care Committee and the Institutional Animal Care and Use Committee (IACUC), and conforms to the National Institutes of Health guidelines for use of animals in research. Thirty two male spontaneously hypertensive rats (SHR; 280–300 g of body weight) were subjected to 90 min occlusion of the right MCA [16]. SHR was used in compliance with the Stroke Therapy Academic Industry Roundtable (STAIR) criteria which explicitly require the use of animals with co-morbid conditions in order to increase the quality of translational stroke research [21].

The two groups studied, the nVNS treated group (n = 16) and the control treated group (n = 16), were determined by a random number generator (www.randomizer.com). Rats in each group were followed for 24 h after reperfusion. A non-invasive stimulator, gammaCore (electroCore, LLC, Basking Ridge, NJ, USA), modified for rat was used for cervical vagus nerve stimulation as described previously [10]. Briefly, after MCAO onset, an electrolyte gel (Signa gel, Parker Laboratories, Fairfield, NJ) was applied to surfaces of the disc electrodes which were then placed on the shaved neck of the rat lateral to the trachea and over the left cervical vagus nerve for the nVNS group, or on the shaved left femur for the control group. After 30 min of occlusion, the rats in the nVNS group received a total of 5, 2 min duration stimulations, one every 10 min. The signal consisted of 1 msec duration pulses of 5 kHz sinewaves, repeated at 25 Hz at an average voltage of 15 V, as described previously [10,18], before reperfusion after 90 min of MCAO. The rats in the control group received the same series of stimulations delivered on the shaved skin overlying the left quadriceps femoris muscle. All procedures, including nVNS or femoris muscle stimulation, were performed under anesthesia with 2% isoflurane during the 90 min occlusion (Fig. 1a), which excluded any neuroprotective effect of isoflurane during cerebral ischemia [22]. In this study, in order to obtain similar outcomes of nVNS neuroprotection on infarct size, we duplicated the procedure of nVNS in previous studies [5,10], which monitored the physiological status of the rats during stimulation and performed behavioral assessment.

Magnetic resonance imaging (MRI)

Twenty rats (n = 10 in nVNS and control group, respectively) were subjected to T2 imaging and dynamic permeability imaging at 24 h after reperfusion as described previously [1,2].

T2-weighted images were acquired with a fast spin-echo sequence (RARE) (TR/TE = 5000ms/56ms, FOV = 4cm×4cm, slice thickness = 1 mm, interslice distance = 1.1 mm, number of slice = 12, matrix = 256 × 256, number of average = 3). Infarct area was manually delineated from T2 images. The delineated areas were used as a reference for all other parametric images. The same slice location was prescribed for all the subsequent MR protocols.

Dynamic contrast-enhanced (DCE)-MRI with graphical analysis was used to non-invasively evaluate BBB permeability [23]. The contrast agent, gadopentetate dimeglumine (Gd)-DTPA, was injected into the femoral vein at a dose of 0.1mM/kg. DCE-MRI was performed using a transverse fast T1 mapping that consisted of obtaining precontrast (3 sequences) and postcontrast (16 sequences) images up to 45 min after the contrast injection. The details of pulse sequence T1_EPI for T1 mapping are: FOV = 4cm×4cm, slice thickness = 1.5mm, slice gap = 0, matrix size = 128 × 128, TR/TE = 10000ms/8.3 ms, number of segment = 4, number of average = 1, total scan time = 2m40s0ms. T1 map was reconstructed with the t1epia fitting function in Bruker Paravision Image Sequence Analysis (ISA) Tool. Since the contrast agent concentration is proportional to changes of $1/T1(\Delta(1/T1(t)))$, a map of K_i was constructed from repeated estimates of $\Delta(1/T1(t))$. An in-house computer program in MATLAB (Mathworks; MA, USA), which implemented the above principle, was used to generate the K_i map.

All data analyses in this study were performed by blinded investigators.

Immunohistochemistry (IHC)

After the MRI scan, animals were sacrificed and rat brains were removed and fixed with 2% paraformaldehyde, 0.1M sodium periodate, 0.075 M lysine in 100 mM phosphate buffer, pH 7.3 (PLP). Ten μm sections were used for immunohistochemical analysis. Primary antibodies and dilutions used in IHC were claudin-5 (1:500) (Invitrogen, Grand Island, NY, USA), occludin (1:500) (Invitrogen), zonula occludens-1 (ZO-1) (1:200, Invitrogen), MMP-2 (1:300, Millipore, Billerica, MA, USA), MMP-9 (1:1000; Millipore), RECA1 (1:300, Abcam, Eugene, OR, USA), glial fibrillary acidic protein (GFAP) (1:400, Sigma-Aldrich, St Louis, MO, USA; 1:100, Abcam).

For immunofluorescence, brain sections were treated with acetone and blocked with 5% normal serum. Primary antibodies were incubated for 48 h at 4 °C. Sections were incubated for 90 min at 25 °C with secondary antibodies conjugated with FITC or Cy-3 (Invitrogen) or cy5 (Santa Cruz, Santa Cruz, CA, USA). 4′-6-diamidino-2-phenylinidole (DAPI) (Molecular Probes, Eugene, OR, USA) was used to label cell nuclei. Immunohistochemistry (IHC) negative controls were incubated without the primary antibody or with normal (non-immune) IgGs and no specific immunolabeling was detected. All IHC slides were viewed on an Olympus BX-51 bright field and fluorescence microscope (Olympus America Inc. San Jose, CA, USA). Dual or triple immunofluorescence slides were also imaged with a Nikon

ECLPSE Tis Inverted Microscope capable of 3D (motorized XY stage and Z focus) Imaging Stitching for both Bright-filed and Single Wave-length/filter cube Epi-Fluor and software (Nikon Instruments Inc. Melville, NY, USA).

Western blot

In a seprate group of rats (n = 6 in both nVNS and control groups), brain tissues were taken to perform Western blot analysis to determine protein levels. Proteins were extracted in RIPA buffer from ischemic and nonischemic hemispheres. 50 μg total protein was separated on 4–10% gradient SDS-PAGE gels (Bio-Rad). The proteins were transferred to polyvinylidene fluoride (PVDF) membranes. The membranes were then incubated with primary antibodies: ZO-1 (1:500, Invitrogen), MMP-2 (1:300, Millipore), MMP-9 (1:1000, Millipore). The membranes were incubated with the respective secondary antibodies and blots were developed using the West Pico Detection System (Pierce). Protein bands were visualized on X-ray film. Semiquantitation of target protein intensities was done with the use of Scion image software (Scion), and blots for β-actin (Sigma-Aldrich) on the same PVDF membranes was used to normalize protein loading and transfer. The results are reported as normalized band intensity for quantifying relative protein expression.

Statistical analysis

Statistical analysis was performed using Prism, version 6.0 (GraphPad Software Incorporated). Unpaired t-tests or one-way ANOVA were performed for two groups or for multiple group comparisons (with a post-hocStudent-Newman-Keuls test), respectively. Linear regression was used for determining the relationship between BBB permeability and infarct size. In all statistical tests, differences were considered significant when $p < 0.05$. Data are presented as means ± SE.

Results

nVNS significantly protected rat brain from ischemic injury by significantly reducing infarct size

T2-weighted images showing hyper-intensity indicate the lesion areas in ipsilateral (ischemic) hemispheres (Fig. 1b). To exclude the influence of swelling, the infarct volumes were normalized with an edema index that was calculated as the volume ratio of ischemic/contralateral (nonischemic) hemispheres [2] (mean ± SEM: 1.149 ± 0.02743 in the control group (CTRL), and 1.107 ± 0.02522 in the nVNS group, n = 10 in each group). Compared with the control group, the nVNS group (control vs. nVNS: 0.1605 ± 0.01881 vs. 0.08906 ± 0.02137, $p < 0.05$, n = 10) showed significant reduction of infarct volume (45.9%) at 24 h after MCAO/reperfusion onset (Fig.1c and d), similar to previous findings [10]. We also evaluated the injury using intensity values from the T2 map (Fig. 1d), which showed a similar outcome with the infarct volume (control vs. nVNS: 85.60 ± 4.727 vs. 54.05 ± 11.18, $p < 0.05$, n = 10). T2-weighted images (Fig. 1a) also demonstrated that the primary region that was protected by nVNS was the cortex, including dorsal, lateral, and piriform areas.

nVNS significantly reduced BBB leakage induced by ischemic stroke

Increased BBB permeability (K_i, indicates BBB transfer rate) was seen in the ischemic hemisphere in the control group compared with the nonischemic hemisphere at 24 h after MCAO/reperfusion onset (Fig. 2a). nVNS significantly decreased the BBB leakage in the lesion area at 24 h compared with control (control vs. nVNS: 6.203e-5 ± 1.202e-5 vs. 3.241e-5 ± 4.344e-6, $p < 0.05$, $n = 10$ in control, 9 in nVNS. One rat in the nVNS group was eliminated due to injection failure of Gd.) (Fig. 2a and b). In line with the BBB K_i maps, significantly lower serum IgG leakage stained with IHC was seen in the ischemic hemisphere (Fig. 2b and c). Notably, the areas and intensities of BBB leakage by IgG IHC were correlated with the BBB leakage presented by the MRI K_i map.

Regression analysis showed that nVNS resulted in a significant correlation ($R^2 = 0.5571$, $p < 0.05$, $n = 9$) between infarct size volume (by T2) and BBB transfer rate (K_i) (by DCE-MRI) in ischemic lesion areas, while the control group showed no correlation ($R^2 = 0.0031$, $p > 0.05$, $n = 10$). These results suggest that the reduction of infarct size by nVNS applied during the occlusion of MCA spatially correlates with the protection of BBB integrity from damage. (Fig. 2d).

nVNS during occlusion protected TJPs in vessel from disruption in ischemic hemisphere

In nonischemic vessels, TJP ZO-1 in the endothelial cells (RECA-1, a marker of endothelial cells) had a linear appearance in both groups (Fig. 3a, left panels), which is typical in normal BBB [16]. In control animals, MCAO and reperfusion disrupted ZO-1, causing a loss from the vascular endothelial cells in the ischemic hemisphere (Fig. 3a, top right panel). In the nVNS treated animals, a much higher RECA-1 signal of endothelial ZO-1 was detected in compromised vessels of ischemic hemispheres (Fig. 3a, right panels). Expression of occludin and claudin-5 in endothelial cells showed similar results with ZO-1 (data not shown). Western blot analysis demonstrated a significant decrease of ZO-1 level in ischemic hemisphere, which was significantly improved by nVNS (Fig. 3b).

nVNS during occlusion reduced expression of MMP-2 and -9 in reactive astrocytes surrounding injured vessels in ischemic hemisphere

Immunohistochemistry also demonstrated that MCAO and reperfusion increased expression of MMP-2 and -9 in cells surrounding the vessels in ischemic areas in both groups, but a few with co-localization of MMP-2 and -9 in endothelial cells were seen (Fig. 4a and b). Importantly, nVNS reduced MMP-2 and -9 in the ischemic areas. Double-immunostaining showed that the cells that express MMP-2 and -9 in ischemic regions at an early stage of reperfusion after MCAO are predominantly found in astrocytes (Fig. 5), and neuronal cells [16,24]. These enzymes have been shown to be involved in BBB disruption and neuronal death. nVNS reduced both expression of MMP-2/-9 and activated astrocytes surrounding the injured vessels in the entire ischemic regions (Fig. 5a and b). Western blot analysis demonstrated a significant increase in MMP-2, including pro- (68 kD) and active (62 kD) forms, and pro-MMP-9 (92 and 88 kD) levels in ischemic hemisphere, which were significantly reduced by nVNS (Fig. 5c and d).

In addition, increased expression of both MMP-2 and in particular MMP-9, were seen in the ischemic external capsule (Fig. 6a and b) where high IgG leakage was observed (Fig. 2c). The major MMP-2 and -9 increases in ECs were not co-localized with GFAP, suggesting these MMPs were expressed in oligodendrocyte-like cells and neurofibrils, which are involved in oligodendrocyte death and white matter damage induced by ischemic stroke [25]. nVNS also attenuated expression of MMPs in white matter.

Discussion

We show that nVNS applied during occlusion of MCA significantly reduced BBB permeability and serum IgG leakage at 24 h after transient ischemic stroke onset. This protection of nVNS on BBB integrity is spatially in line with the attenuation of the infarct size in the ischemic hemispheres. Histological evaluation in this study also indicated that the nVNS mediated protection of BBB from breakdown is associated with reduction of MMP-mediated TJP disruption. We propose that nVNS attenuates MMP-mediated BBB damage during the early ischemic insult, which results in reduction of cell death, neuroinflammation, and infarct size in ischemic brain secondary to BBB disruption.

The neurological outcomes in patients suffering from cerebral ischemia depends on the intensity of hypoxia and the extent of secondary brain injury. Therefore, therapeutic approaches for acute ischemic stroke are highly needed. Recent studies demonstrate that VNS reduces ischemic stroke induced brain injury in rats and improves neurological outcomes [5,8,10,26]. These studies indicate that stimulation of vagus nerve both during MCA occlusion and at an early reperfusion stage significantly reduces brain injury and functional neurological deficit. The decrease in tissue damage was accompanied by a significant improvement in neurological scores. Physiological parameters for safety analysis showed no difference in arterial blood pressure, heart rate, arterial blood gases and pH, symptomatic brain hemorrhage, and mortality or development of any of the euthanasia criteria between control and treatment groups [5,10]. There was no significant effect of VNS on CBF during the entire 1-h stimulation period [8]. These observations open up new possibilities for early neuroprotective strategies dealing with ischemia and reperfusion-based injury. To better understand the mechanisms involved in stroke-induced BBB pathology we applied nVNS to rats during occlusion of the middle cerebral artery, since increased BBB permeability occurs as early as 1–2 h after MCAO onset [15,27]. nVNS has been shown to reduce the extent of tissue injury and functional deficit in SH rats without causing cardiac or hemodynamic adverse effects when initiated up to 4 h after MCAO [10]. Therefore, nVNS could be provided to stroke patients as early as when they are transferred to the hospital in an ambulance. We used non-invasive MRI to monitor the outcome of control and nVNS-treated ischemic brains. T2 anatomical imaging showed significant protection from brain infarct extent with nVNS compared with control at 24 h after stroke onset. nVNS demonstrated a 45.9% decrease in total infarct volume in rat brain subjected to 90 min MCAO as measured on T2-weighted images [1]. This is similar to previous reports (~45–56% reduction) using cervical vagus nerve stimulation (iVNS) [5,8,26], but larger than previously reported reductions achieved by nVNS (33%) [10]. Since SHRs and nVNS were used in both the previous [10] and present studies, this discrepancy could be due to different measurement techniques for infarct volume and the endpoints of occlusion/reperfusion, i.e.

post-mortem rat brain by triphenyl tetrazolium chloride (TTC) staining at 7 days after 120 min MCAO vs. living rat brain by MRI at 24 h after 90 min of MCAO. In addition, our data also demonstrate that nVNS, contralateral to occlusion of MCA, can provide protection to rat brain from acute focal ischemic injury, consistent with potential mechanisms of VNS which are known to activate central and peripheral pathways, bilaterally [8,11,12,28].

Although the nVNS neuroprotective role against acute cerebral ischemia is clear, the underlying mechanisms by which VNS enhances recovery following stroke remain to be fully elucidated. Data from previous studies have suggested several mechanisms underlying VNS-mediated neuroprotection in neurological disorders, including a noradrenergic mechanism, anti-inflammation, reduction in neuronal excitability, and regional brain perfusion changes [3,4,11,12,28–32]. A study of traumatic brain injury (TBI) showed that VNS attenuated BBB permeability by decreasing the up-regulation of aquaporin-4, a water permeable channel, after TBI [33]. Disruptions of the BBB and edema formation both play key roles in the development of neurological dysfunction in ischemic and hemorrhagic stroke, TBI, neurodegenerative diseases and brain tumors [14,34]. During and after ischemic stroke, BBB breakdown and the resulting brain edema are two of the most disabling sequelae and are associated with poor clinical prognosis [14,27,35]. Notably, the progression of stroke is correlated with BBB breakdown [36]. We and others have demonstrated that early BBB permeability may be partially reversible, making it a rational target for therapeutic interventions [1,2,14,16,27]. This study shows that nVNS applied during occlusion of MCAO significantly reduces BBB permeability induced by ischemia and reperfusion at 24 h after stroke as measured by DCE-MRI. This finding is consistent with the patterns of significantly lower serum IgG leakage in ischemic hemispheres of nVNS-treated rats detected with IHC after MRI. We and others [16,37,38] have shown changes of BBB integrity and related pathogenic processes in contralateral brain areas, which was also observed in this study, and nVNS showed protective changes for the contralateral side as well. This observation may bring into question the use of our edema index ratio correction for swelling. However, there was no statistical difference in the contralateral hemisphere volumes between the control and nVNS groups in spite of a small change in BBB permability.

We found that the reduction of infarct volume by applying nVNS at 30 min of occlusion of MCA onset significantly correlates with the protection of BBB integrity from damage. We did not detect, however, a correlation between infarct volume and BBB leakage in control rats. One of the possible reasons could be that up to 24 h after stroke/reperfusion onset, besides the BBB opening, other pathological factors, such as inflammatory responses, are involved in the extent of infarct severity and that nVNS may have a significant protective effect against them. Indeed, in a very similar rat model, Ay et al. showed that nVNS reduced the number of activated microglia at 24 h and the number of cells expressing inflammatory cytokines like TNF-α compared with control at 3 and/or 24 h after stroke/reperfusion onset[9]. Collectively, our data present another potential mechanism involved in neuroprotection of VNS on BBB disruption, during stroke-induced brain injury.

The integrity of the BBB is maintained by multiple components, including the tight junction (TJ)-sealed capillary ECs, astrocyte endfeet, pericytes and the extracellular matrix (ECM)

[34]. The limited permeability of the BBB is mainly due to the existence of TJs. Tight junction proteins are integral transmembrane proteins that form the TJ strands between endothelial cells. Prominent BBB structural changes occur after cerebral ischemic stroke, including TJP degradation and redistribution [34,39]. A number of mechanisms have been proposed to account for the degradation of TJPs. Matrix metalloproteinases are degrading enzymes that can disrupt the TJPs, leading to the BBB disruption during ischemic stroke and after reperfusion [16,40]. In reperfusion injury, proteases participate in the biphasic opening of the BBB. An initial reversible phase related to activation of latent MMP-2 precedes a later phase at 24–48 h associated with the induction of MMP-3 and MMP-9 [16,41]. As seen in our data, nVNS prevented BBB from disruption as evidenced by histologic changes including decreased TJP cleavage, including ZO-1, occludin, and claudin-5 in endothelial cells, and inhibition of expression of MMP-2 and -9 in reactive astrocytes surrounding injured vessels in the ischemic hemisphere, at 24 h after stroke onset. We have previously shown that ischemia and reperfusion induce reactive astrocytes to express MMP-2 and -9, leading to BBB disruption by cleaving TJPs [16]. The changes of histology and protein levels of TJPs and MMPs by nVNS administration suggest the involvement of MMP activity inhibition in the mechanisms involved in neuroprotection of VNS on BBB disruption during stroke-induced brain injury.

An important caveat is that only one time point was examined at 24 h after stroke onset. Future studies are needed to specifically elucidate the timing duration, especially the early stages (such as 30 min, 3 h, and 6 h after reperfusion), to confirm the involvement of the protective role of nVNS on BBB disruption induced during the early stages of stroke insult. In addition, using the multimodal MRI we can determine if the promising results obtained in this study extend to chronic neuroprotection. In order to obtain similar outcomes of nVNS neuroprotection on infarct size, we employed the procedure of nVNS in previous studies [5,10] to determine if the neuroprotective role of nVNS on infarct size correlated with protection of BBB integrity from damage. Since the previous studies performed behavioral assessment, we did not do it in the present study. However, a battery of neurological/behavioral tests should be involved in the future longitudinal evaluation of the nVNS role on neuroprotection in stroke insult. Other limitations of the study are a lack of monitoring of blood flow to confirm adequate MCAO, and monitoring of various physiological parameters like blood pressure, heart rate, and temperature, all of which can have an impact on stroke severity. However, the fact that the reduction of infarct volume (45.9%) in nVNS group at 24 h of reperfusion in the present study was similar to those reported previously (~45–56%) [5,8,26], suggests that these limitations had only minimal effects on the results.

Conclusions

The present results suggest that the neuroprotective role of a series of nVNS administrations during MCA occlusion correlates with protection of BBB integrity from damage induced by ischemic stroke. The mechanism likely involves protecting the BBB by reducing MMP-mediated TJP disruption. The more precise cellular and molecular pathways regulated by nVNS, including BBB integrity changes, inflammatory responses, and cell death and survival, should be further studied at multiple time points during the early stage after reperfusion. A recent study demonstrated that rapid endothelial cytoskeletal reorganization

induces subtle BBB leakage by inducing TJP redistribution in brain microvascular endothelial cells within 30–60 min after perfusion [27]. It is possible that the rapid endothelial cytoskeletal reorganization could also be a target of nVNS administration during MCA occlusion.

Acknowledgments

Funding sources

This work was supported in part by electroCore, LLC unrestricted gift, grants from National Institution of Health (1R21 NS091710) and American Heart Associationt (13GRNT17060032) to Dr. Yi Yang.

References

1. Yang Y, Salayandia VM, Thompson JF, Yang LY, Estrada EY, Yang Y. Attenuation of acute stroke injury in rat brain by minocycline promotes blood-brain barrier remodeling and alternative microglia/macrophage activation during recovery. J Neuroinflammation. 2015; 12:26. [PubMed: 25889169]
2. Yang Y, Thompson JF, Taheri S, Salayandia VM, McAvoy TA, Hill JW, et al. Early inhibition of MMP activity in ischemic rat brain promotes expression of tight junction proteins and angiogenesis during recovery. J Cereb blood Flow Metab. 2013; 33:1104–14. [PubMed: 23571276]
3. Ben-Menachem E, Revesz D, Simon BJ, Silberstein S. Surgically implanted and non-invasive vagus nerve stimulation: a review of efficacy, safety and tolerability. Eur J Neurol. 2015; 22:1260–8. [PubMed: 25614179]
4. Neren D, Johnson MD, Legon W, Bachour SP, Ling G, Divani AA. Vagus nerve stimulation and other neuromodulation methods for treatment of traumatic brain injury. Neurocrit Care. 2016; 24:308–19. [PubMed: 26399249]
5. Ay I, Lu J, Ay H, Gregory Sorensen A. Vagus nerve stimulation reduces infarct size in rat focal cerebral ischemia. Neurosci Lett. 2009; 459:147–51. [PubMed: 19446004]
6. Beekwilder JP, Beems T. Overview of the clinical applications of vagus nerve stimulation. J Clin Neurophysiol. 2010; 27:130–8. [PubMed: 20505378]
7. Vonck K, Raedt R, Naulaerts J, De Vogelaere F, Thiery E, Van Roost D, et al. Vagus nerve stimulation…25 years later! what do we know about the effects on cognition? Neurosci Biobehav Rev. 2014; 45:63–71. [PubMed: 24858008]
8. Ay I, Sorensen AG, Ay H. Vagus nerve stimulation reduces infarct size in rat focal cerebral ischemia: an unlikely role for cerebral blood flow. Brain Res. 2011; 1392:110–5. [PubMed: 21458427]
9. Silberstein SD, Mechtler LL, Kudrow DB, Calhoun AH, McClure C, Saper JR, et al. Non-invasive vagus nerve stimulation for the ACute treatment of cluster headache: findings from the randomized, double-blind, sham-controlled ACT1 study. Headache. 2016; 56:1317–32. [PubMed: 27593728]
10. Ay I, Nasser R, Simon B, Ay H. Transcutaneous cervical vagus nerve stimulation ameliorates acute ischemic injury in rats. Brain Stimul. 2016; 9:166–73. [PubMed: 26723020]
11. Bonaz B, Sinniger V, Pellissier S. Anti-inflammatory properties of the vagus nerve: potential therapeutic implications of vagus nerve stimulation. J Physiol. 2016; 594:5781–90. [PubMed: 27059884]
12. Duris K, Lipkova J, Jurajda M. Cholinergic anti-inflammatory pathway and stroke. Curr Drug Deliv. 2017; 14:449–57. [PubMed: 28155595]
13. Yan FL, Zhang JH. Role of the sympathetic nervous system and spleen in experimental stroke-induced immunodepression. Med Sci Monit. 2014; 20:2489–96. [PubMed: 25434807]
14. Yang Y, Rosenberg GA. Blood-brain barrier breakdown in acute and chronic cerebrovascular disease. Stroke. 2011; 42:3323–8. [PubMed: 21940972]

15. Jin X, Liu J, Yang Y, Liu KJ, Yang Y, Liu W. Spatiotemporal evolution of blood brain barrier damage and tissue infarction within the first 3h after ischemia onset. Neurobiol Dis. 2012; 48:309–16. [PubMed: 22813865]
16. Yang Y, Estrada EY, Thompson JF, Liu W, Rosenberg GA. Matrix metalloproteinase-mediated disruption of tight junction proteins in cerebral vessels is reversed by synthetic matrix metalloproteinase inhibitor in focal ischemia in rat. J Cereb blood Flow Metab. 2007; 27:697–709. [PubMed: 16850029]
17. Oshinsky ML, Murphy AL, Hekierski H Jr, Cooper M, Simon BJ. Noninvasive vagus nerve stimulation as treatment for trigeminal allodynia. Pain. 2014; 155:1037–42. [PubMed: 24530613]
18. Chen SP, Ay I, de Morais AL, Qin T, Zheng Y, Sadeghian H, et al. Vagus nerve stimulation inhibits cortical spreading depression. Pain. 2016; 157:797–805. [PubMed: 26645547]
19. Akerman S, Simon B, Romero-Reyes M. Vagus nerve stimulation suppresses acute noxious activation of trigeminocervical neurons in animal models of primary headache. Neurobiol Dis. 2017; 102:96–104. [PubMed: 28286178]
20. Cai PY, Bodhit A, Derequito R, Ansari S, Abukhalil F, Thenkabail S, et al. Vagus nerve stimulation in ischemic stroke: old wine in a new bottle. Front Neurol. 2014; 5:107. [PubMed: 25009531]
21. Fisher M, Feuerstein G, Howells DW, Hurn PD, Kent TA, Savitz SI, et al. Update of the stroke therapy academic industry roundtable preclinical recommendations. Stroke. 2009; 40:2244–50. [PubMed: 19246690]
22. Taheri S, Shunmugavel A, Clark D, Shi H. Isoflurane reduces the ischemia reperfusion injury surge: a longitudinal study with MRI. Brain Res. 2014; 1586:173–83. [PubMed: 25124744]
23. Patlak CS, Blasberg RG, Fenstermacher JD. Graphical evaluation of blood-to-brain transfer constants from multiple-time uptake data. J Cereb Blood Flow Metab. 1983; 3:1–7. [PubMed: 6822610]
24. Yang Y, Candelario-Jalil E, Thompson JF, Cuadrado E, Estrada EY, Rosell A, et al. Increased intranuclear matrix metalloproteinase activity in neurons interferes with oxidative DNA repair in focal cerebral ischemia. J Neurochem. 2010; 112:134–49. [PubMed: 19840223]
25. Yang Y, Jalal FY, Thompson JF, Walker EJ, Candelario-Jalil E, Li L, et al. Tissue inhibitor of metalloproteinases-3 mediates the death of immature oligodendrocytes via TNF-alpha/TACE in focal cerebral ischemia in mice. J Neuroinflammation. 2011; 8:108. [PubMed: 21871134]
26. Sun Z, Baker W, Hiraki T, Greenberg JH. The effect of right vagus nerve stimulation on focal cerebral ischemia: an experimental study in the rat. Brain Stimul. 2012; 5:1–10. [PubMed: 22037134]
27. Shi Y, Zhang L, Pu H, Mao L, Hu X, Jiang X, et al. Rapid endothelial cytoskeletal reorganization enables early blood-brain barrier disruption and long-term ischaemic reperfusion brain injury. Nat Commun. 2016; 7:10523. [PubMed: 26813496]
28. Pavlov VA, Tracey KJ. Neural regulation of immunity: molecular mechanisms and clinical translation. Nat Neurosci. 2017; 20:156–66. [PubMed: 28092663]
29. Follesa P, Biggio F, Gorini G, Caria S, Talani G, Dazzi L, et al. Vagus nerve stimulation increases norepinephrine concentration and the gene expression of BDNF and bFGF in the rat brain. Brain Res. 2007; 1179:28–34. [PubMed: 17920573]
30. Borovikova LV, Ivanova S, Zhang M, Yang H, Botchkina GI, Watkins LR, et al. Vagus nerve stimulation attenuates the systemic inflammatory response to endotoxin. Nature. 2000; 405:458–62. [PubMed: 10839541]
31. Neese SL, Sherill LK, Tan AA, Roosevelt RW, Browning RA, Smith DC, et al. Vagus nerve stimulation may protect GABAergic neurons following traumatic brain injury in rats: an immunocytochemical study. Brain Res. 2007; 1128:157–63. [PubMed: 17125748]
32. Schweighofer H, Rummel C, Roth J, Rosengarten B. Modulatory effects of vagal stimulation on neurophysiological parameters and the cellular immune response in the rat brain during systemic inflammation. Intensive Care Med Exp. 2016; 4:19. [PubMed: 27357828]
33. Lopez NE, Krzyzaniak MJ, Costantini TW, Putnam J, Hageny AM, Eliceiri B, et al. Vagal nerve stimulation decreases blood-brain barrier disruption after traumatic brain injury. J Ttrauma Acute Care Surg. 2012; 72:1562–6.

34. Neuwelt EA, Bauer B, Fahlke C, Fricker G, Iadecola C, Janigro D, et al. Engaging neuroscience to advance translational research in brain barrier biology. Nat Rev Neurosci. 2011; 12:169–82. [PubMed: 21331083]

35. Khatri R, McKinney AM, Swenson B, Janardhan V. Blood-brain barrier, reperfusion injury, and hemorrhagic transformation in acute ischemic stroke. Neurology. 2012; 79:S52–7. [PubMed: 23008413]

36. Brouns R, Wauters A, De Surgeloose D, Marien P, De Deyn PP. Biochemical markers for blood-brain barrier dysfunction in acute ischemic stroke correlate with evolution and outcome. Eur Neurol. 2011; 65:23–31. [PubMed: 21135557]

37. Sbarbati A, Reggiani A, Nicolato E, Arban R, Lunati E, Osculati F. Regional changes in the contralateral “healthy” hemisphere after ischemic lesions evaluated by quantitative T2 parametric maps. Anato Rec. 2002; 266:118–22.

38. Garbuzova-Davis S, Rodrigues MC, Hernandez-Ontiveros DG, Tajiri N, Frisina-Deyo A, Boffeli SM, et al. Blood-brain barrier alterations provide evidence of subacute diaschisis in an ischemic stroke rat model. PLoS One. 2013; 8:e63553. [PubMed: 23675488]

39. Krueger M, Bechmann I, Immig K, Reichenbach A, Hartig W, Michalski D. Blood-brain barrier breakdown involves four distinct stages of vascular damage in various models of experimental focal cerebral ischemia. J Cereb Blood Flow Metab. 2015; 35:292–303. [PubMed: 25425076]

40. Liu J, Jin X, Liu KJ, Liu W. Matrix metalloproteinase-2-mediated occludin degradation and caveolin-1-mediated claudin-5 redistribution contribute to blood-brain barrier damage in early ischemic stroke stage. J Neurosci. 2012; 32:3044–57. [PubMed: 22378877]

41. Yan J, Li L, Khatibi NH, Yang L, Wang K, Zhang W, et al. Blood-brain barrier disruption following subarchnoid hemorrhage may be faciliated through PUMA induction of endothelial cell apoptosis from the endoplasmic reticulum. Exp Neurol. 2011; 230:240–7. [PubMed: 21586287]

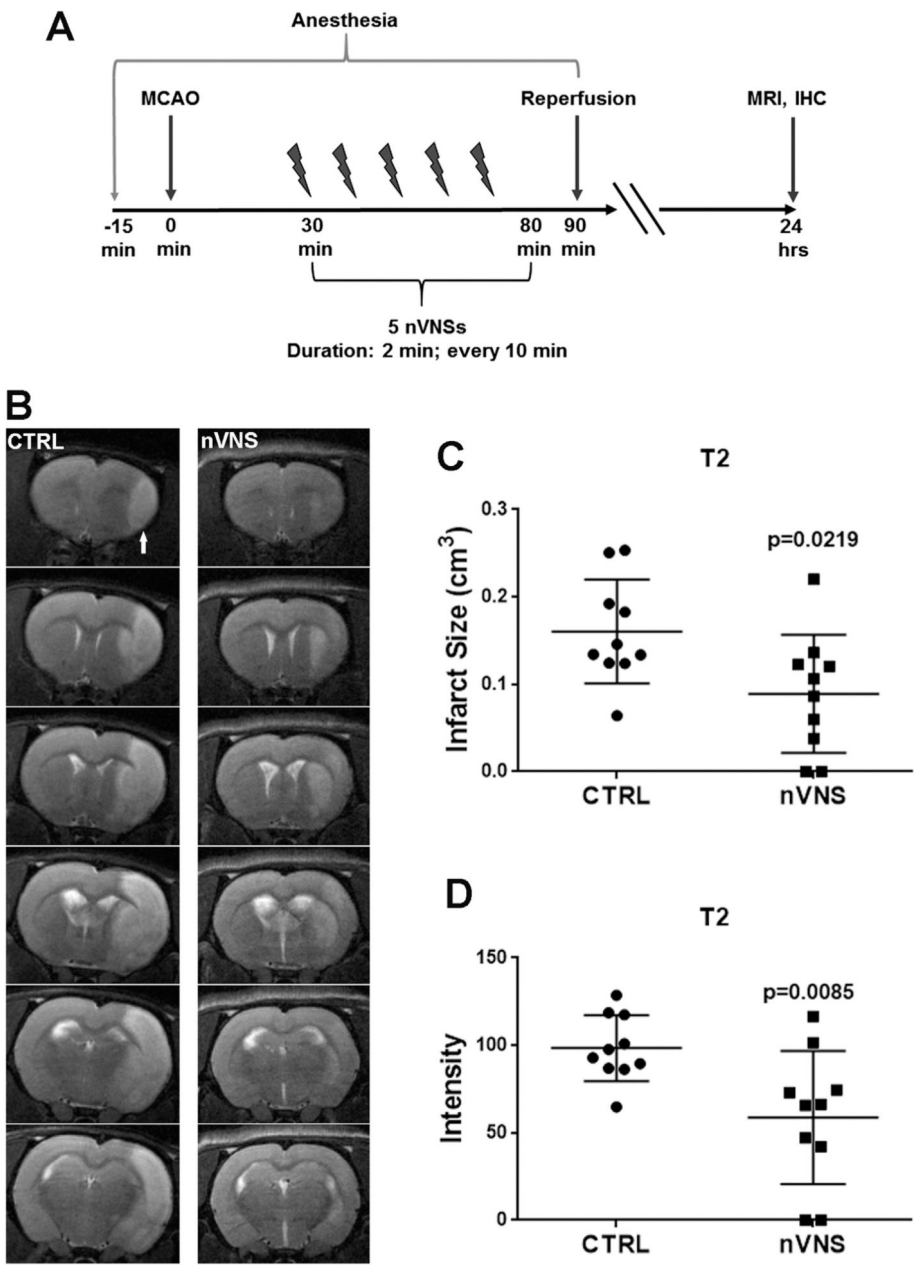

Fig. 1.

Stroke infarct size monitored by magnetic resonance imaging (MRI). **a**. Experimental design for nVNS during MACO. **b.** Anatomical T2 MR images indicate the infarct areas with increased intensity. Arrows indicate ischemic hemispheres. **c**. Bar graph demonstrates quantification of infarct volumes in ischemic hemispheres. $p < 0.05$ versus control (CTRL), $n = 10$ in each group. The infarct volumes were normalized for edema. **d**. Bar graph demonstrates quantification of T2 intensity in ischemic hemispheres. $p < 0.05$ versus control. $n = 10$ in each group.

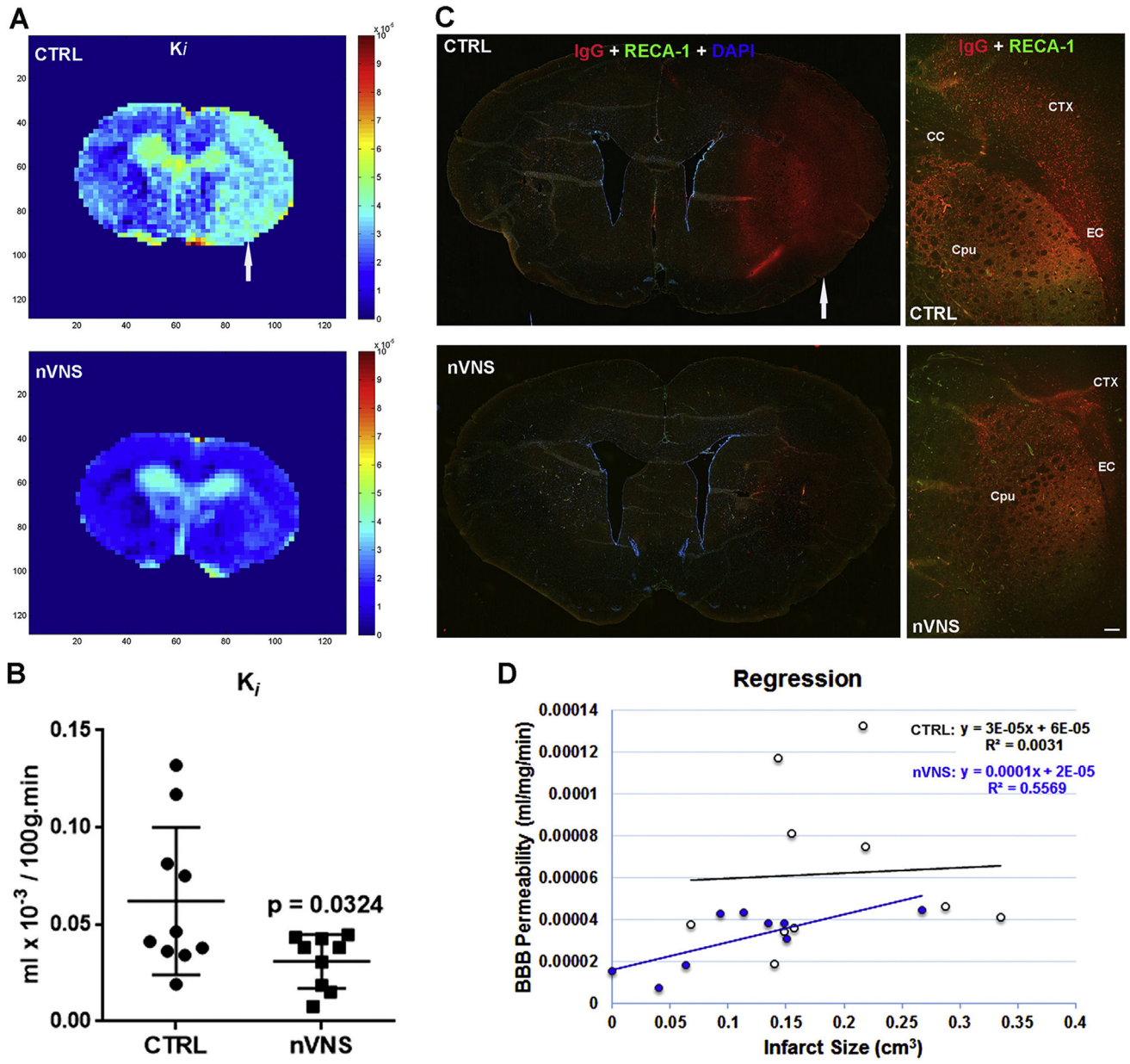

Fig. 2.

BBB permeability of microvessels monitored by DCE-MRI and IgG immunohistochemistry at 24 h after stroke in control and nVNS groups. **a**. Parametric image K_i map by DCE-MRI represents BBB permeability in brains. Arrow indicates ischemic hemisphere. Color-coded permeability coefficient maps reconstructed from contrast-enhanced MRI data demonstrate the regions of high (red) and low (blue) permeability. **b**. Histogram demonstrates quantification of BBB permeability in lesion areas. *p < 0.03 vs. control group. n = 10 in control group, n = 9 in nVNS group (one rat in nVNS group was eliminated due to failure of Gd injection). **c**. Immunohistochemistry of IgG and RECA-1 represent increased BBB leakage in ischemic hemispheres (arrow), corresponding to the regions where increased BBB transfer rate was detected by MRI. DAPI staining was used to show nuclei. Higher

power micrographs show leaked IgG from injured vessels stained brain cells in ischemic hemispheres. CTX: cortex; Cpu: caudoputamen; CC: corpus callosum; EC: external capsule. Scale bar = 50 μm. **d**. Regression analysis between BBB permeability (y-axis) and infarct size (x-axis): CTRL group (black), $R^2 = 0.0031$, $p > 0.05$, n = 10; nVNS group (blue), $R^2 = 0.5571$, $p < 0.05$, N = 9. (For interpretation of the references to colour in this figure legend, the reader is referred to the Web version of this article.)

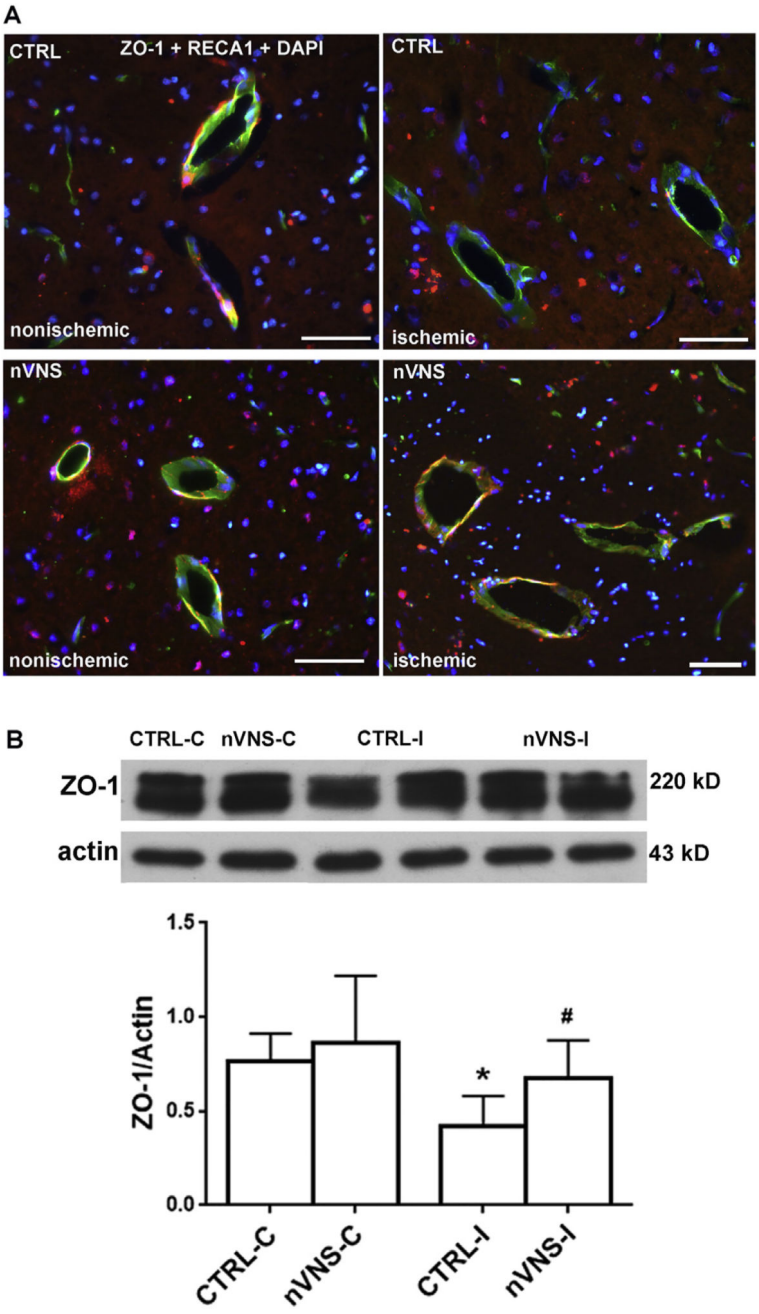

Fig. 3.

Expression of tight junction protein ZO-1 in the vascular endothelial cells (RECA-1) within caudate regions 24 h of reperfusion after MCAO by double immunostaining. **a**. Top panels: co-localization of ZO-1 with RECA-1 in nonischemic and ischemic vessels in control brains. Bottom panels: co-localization of ZO-1 with RECA-1 in nonischemic and ischemic vessels in nVNS treated brains. DAPI staining was used to show nuclei. Scale bars = 50 μm. **b**. Western blot analysis for protein level of ZO-1. *$p < 0.05$ versus CTRL-C, $^{\#}p < 0.05$ versus CTRL-I, n = 6 in each group. C: contralateral. I: ipsilateral.

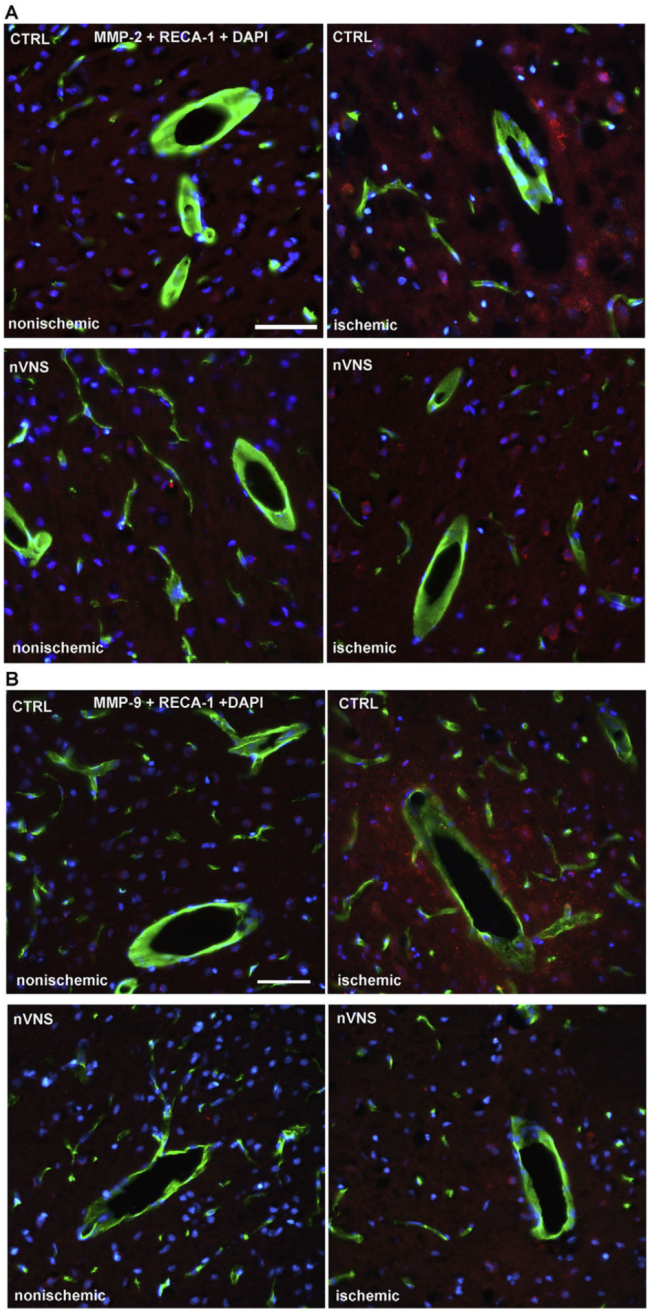

Fig. 4.

Expression of MMP-2 and MMP-9 in the vascular endothelial cells (RECA-1) in nonischemic and ischemic hemispheres 24 h of reperfusion after MCAO by double immunostaining. **a**. Double-immunostaining of MMP-2 with RECA-1 in control and nVNS treated brains. **b**. Double-immunostaining of MMP-9 with RECA-1 in control and nVNS treated brains. DAPI staining was used to show nuclei. Scale bar = 50 μm.

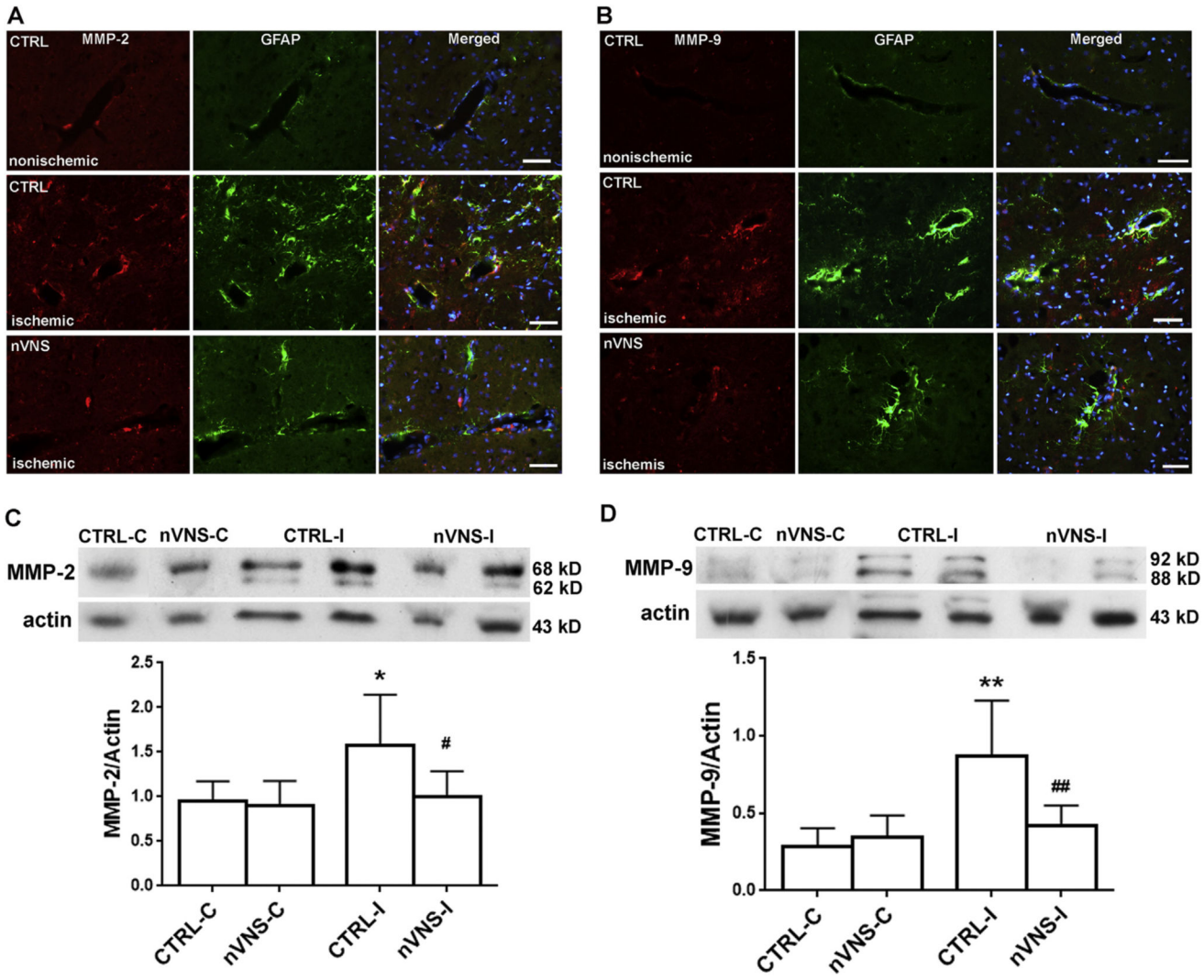

Fig. 5.

Expression of MMP-2 and -9 in the astrocytes (GFAP) in nonischemic and ischemic hemispheres 24 h of reperfusion after MCAO by double immunostaining. **a**. Co-localization of MMP-2 with GFAP in control and nVNS treated brains. **b**. Co-localization of MMP-9 with GFAP in control and nVNS treated brains. DAPI staining was used to show nuclei. Scale bar = 50 μm. **c**. Western blot analysis for protein levels of MMP-2. *$p < 0.05$ versus CTRL-C and nVNS-C, $^{\#}p < 0.05$ versus CTRL-I, n = 6 in each group. **d**. Western blot analysis for protein levels of MMP-9. **$p < 0.01$ versus CTRL-C and nVNS-C, $^{\#\#}p < 0.01$ versus CTRL-I, n = 6 in each group.

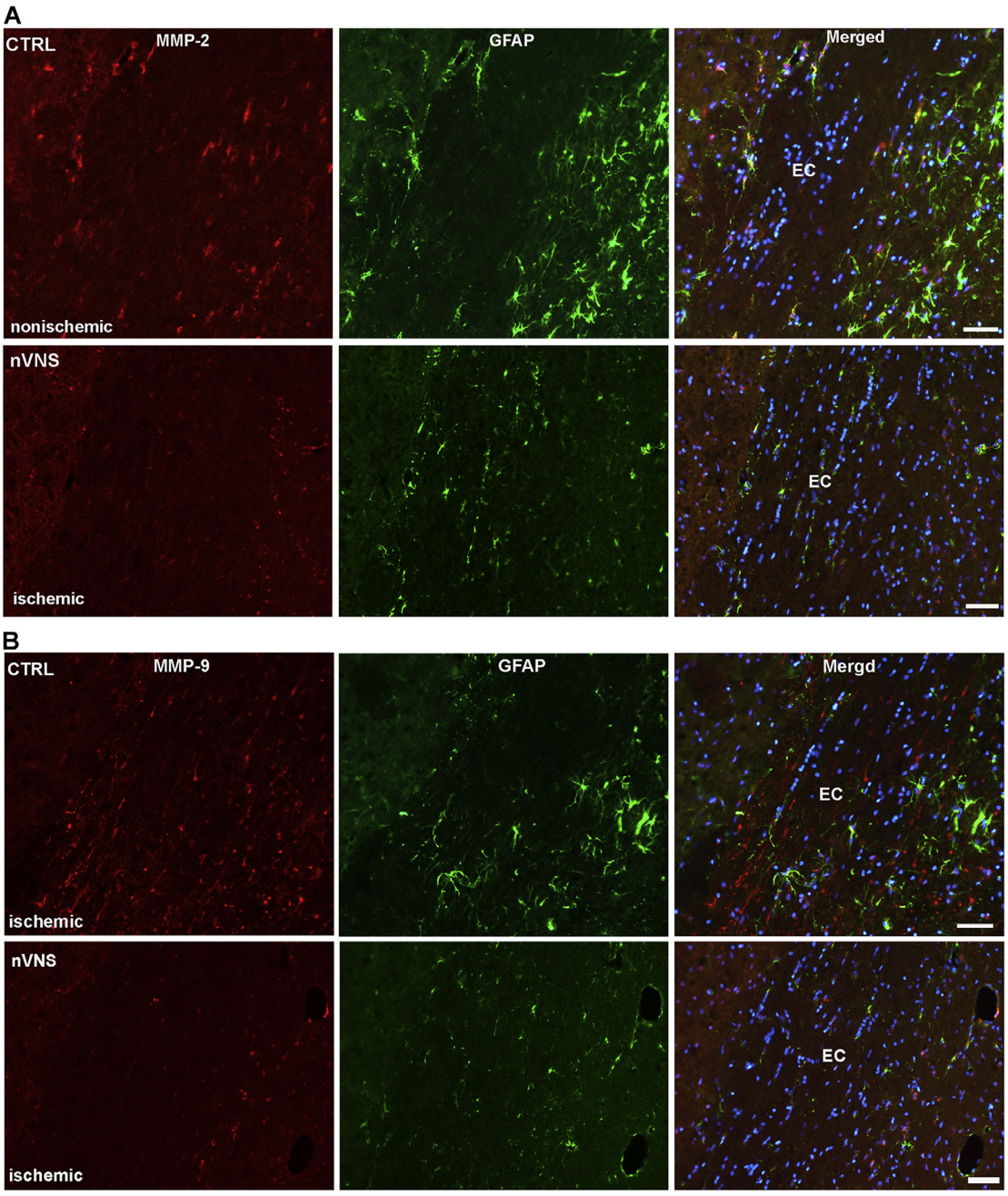

Fig. 6.

Expression of MMP-2 and -9 in astrocytes (GFAP) in nonischemic and ischemic external capsule (EC) 24 h of reperfusion after MCAO by double immunostaining. **a.** Co-localization of MMP-2 with GFAP in control and nVNS treated brains. **b.** Co-localization of MMP-9 with GFAP in control and nVNS treated brains. DAPI staining was used to show nuclei. Scale bar= 50 μm.